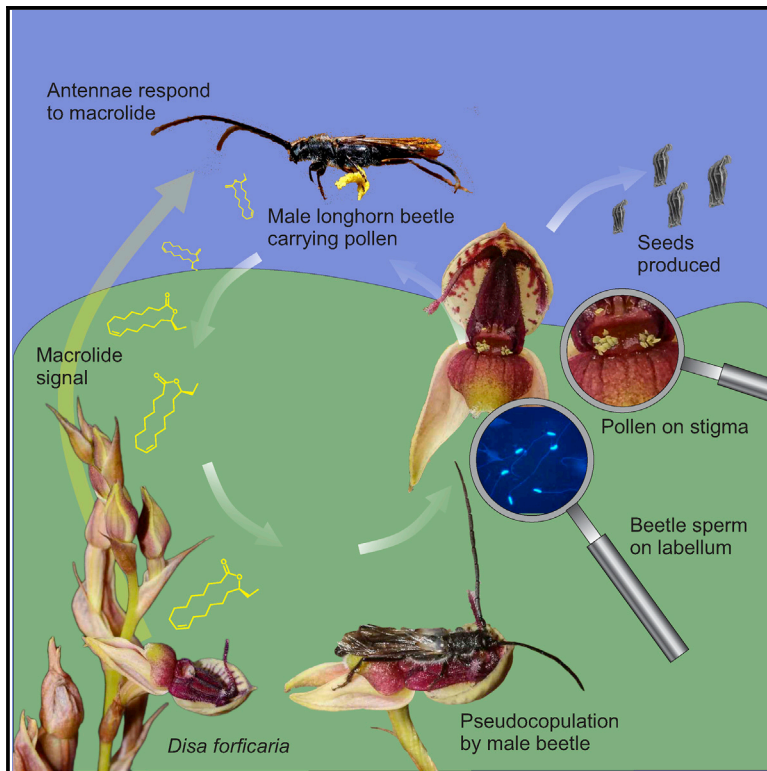


# Current Biology

## Sexual deception of a beetle pollinator through floral mimicry

### Graphical abstract



### Authors

Callan Cohen, William R. Liltved, Jonathan F. Colville, ..., Aleš Svatoš, Benny Bytebier, Steven D. Johnson

### Correspondence

johnsonsd@ukzn.ac.za

### In brief

Cohen et al. report that an African orchid is pollinated by male longhorn beetles, which ejaculate while attempting to copulate with the flowers. They identify a novel macrolide that mediates this system of sexual deception and show that structural geometry of the molecule is critical for attraction of male beetles.

### Highlights

- The critically rare orchid *Disa forficaria* is pollinated by male longhorn beetles
- Male beetles are sexually deceived and ejaculate on the flowers
- Male beetles are attracted by a novel macrolide emitted by the orchid
- Structural geometry of the macrolide is critical for attraction of beetles



## Report

# Sexual deception of a beetle pollinator through floral mimicry

Callan Cohen,<sup>1</sup> William R. Liltved,<sup>2</sup> Jonathan F. Colville,<sup>3,4</sup> Adam Shuttleworth,<sup>5</sup> Jerrit Weissflog,<sup>6</sup> Aleš Svatoš,<sup>6</sup> Benny Bytebier,<sup>5</sup> and Steven D. Johnson<sup>5,7,\*</sup>

<sup>1</sup>FitzPatrick Institute of African Ornithology, DST-NRF Centre of Excellence, University of Cape Town, Rondebosch 7701, South Africa

<sup>2</sup>Compton Herbarium, South African National Biodiversity Institute, Newlands, Cape Town 7735, South Africa

<sup>3</sup>Kirstenbosch Research Centre, South African National Biodiversity Institute, Newlands, Cape Town 7735, South Africa

<sup>4</sup>Statistics in Ecology, Environment and Conservation, Department of Statistical Sciences, University of Cape Town, Rondebosch 7701, South Africa

<sup>5</sup>Centre for Functional Biodiversity, School of Life Sciences, University of KwaZulu-Natal, Private Bag X01, Pietermaritzburg 3209, South Africa

<sup>6</sup>Max Planck Institute for Chemical Ecology, Hans-Knöll-Str. 8, D-07745 Jena, Germany

<sup>7</sup>Lead contact

\*Correspondence: [johnsonsd@ukzn.ac.za](mailto:johnsonsd@ukzn.ac.za)

<https://doi.org/10.1016/j.cub.2021.03.037>

## SUMMARY

Sexual mimicry is a complex multimodal strategy used by some plants to lure insects to flowers for pollination.<sup>1–4</sup> It is notable for being highly species-specific and is typically mediated by volatiles belonging to a restricted set of chemical compound classes.<sup>3,4</sup> Well-documented cases involve exploitation of bees and wasps (Hymenoptera)<sup>5,6</sup> and flies (Diptera).<sup>7–9</sup> Although beetles (Coleoptera) are the largest insect order and are well known as pollinators of both early and modern plants,<sup>10,11</sup> it has been unclear whether they are sexually deceived by plants during flower visits.<sup>12,13</sup> Here we report the discovery of an unambiguous case of sexual deception of a beetle: male longhorn beetles (*Chorothyse hessei*, Cerambycidae) pollinate the elaborate insectiform flowers of a rare southern African orchid (*Disa forficaria*), while exhibiting copulatory behavior including biting the antennae-like petals, curving the abdomen into the hairy lip cleft, and ejaculating sperm. The beetles are strongly attracted by (16S,9Z)-16-ethyl hexadec-9-enolide, a novel macrolide that we isolated from the floral scent. Structure-activity studies<sup>14,15</sup> confirmed that chirality and other aspects of the structural geometry of the macrolide are critical for the attraction of the male beetles. These results demonstrate a new biological function for plant macrolides and confirm that beetles can be exploited through sexual deception to serve as pollinators.

## RESULTS AND DISCUSSION

### Evidence for sexual deception of longhorn beetles

Males of the longhorn beetle *Chorothyse hessei* (Cerambycidae: Cerambycinae) exhibit sexual behavior when visiting flowers of the orchid *Disa forficaria* (Figures 1A, 1G, and 1H). This orchid is endemic to the Cape Floristic Region and is exceedingly rare, with only 11 plants having been recorded in the past two centuries.<sup>16</sup> Its flowers do not produce nectar or any other food reward, and are visited exclusively by *C. hessei*. Visits (11 recorded over 12 days in 2016 and 2018) lasted a mean ( $\pm$ SE) of  $221 \pm 67.2$  s and involved protracted copulatory behavior (Video S1), which included arching the abdomen so that its tip was buried in the hairs at the cleft tip of the lip (Figures 1G, 1H, and 1L) and biting the antennae-like petals (Figures 1G and 1H), actions that are similar to the mating behavior described in other longhorn beetles.<sup>17</sup> Extension of the male sex organ (aedeagus) was clearly visible (Figure 1L) and sperm packages were seen to be deposited within the hairy cleft at the apex of the floral lip after these visits (Figures 1M and 1N). A sample taken from the floral lip immediately after a visit by a beetle was found to contain

large numbers ( $>10,000$ ) of sperm ca. 200  $\mu$ m in length (Figures 1O and 1P). Ejaculation by male insects very rarely occurs during sexual deception by flowers and was previously confirmed only for male ichneumonid wasps deceived by Australian *Cryptostylis* orchids,<sup>18</sup> but is suspected to also occur for fungus gnat pollinators of the South American orchid genus *Lepanthes*.<sup>8</sup>

The sexual behavior described above resulted in effective removal and deposition of pollen. Flowers of *D. forficaria* measure c. 13 mm from the dorsal sepal apex to the lip apex (Figure 1A) and thus closely match the length from the head to the tip of the abdomen of *C. hessei* individuals;  $9.88 \pm 0.26$  mm (mean  $\pm$  SE,  $n = 19$ ) for males captured in this study (Figures 1A, 1G, and 1H) and 12 mm for a female specimen.<sup>19</sup> The beetles place their hind legs on the lateral sepals (Figures 1G and 1L) while their sternum contacts the centrally positioned viscidia (the adhesive bases of the pollinaria) and stigma, resulting in withdrawal of pollinaria (Figures 1I and 1J). Beetles arriving with pollinaria attached to the underside of the thorax (Figures 1I and 1J) were seen to deposit pollen massulae on the stigma (Figure 1K) and these flowers ultimately developed into fully formed fruits.



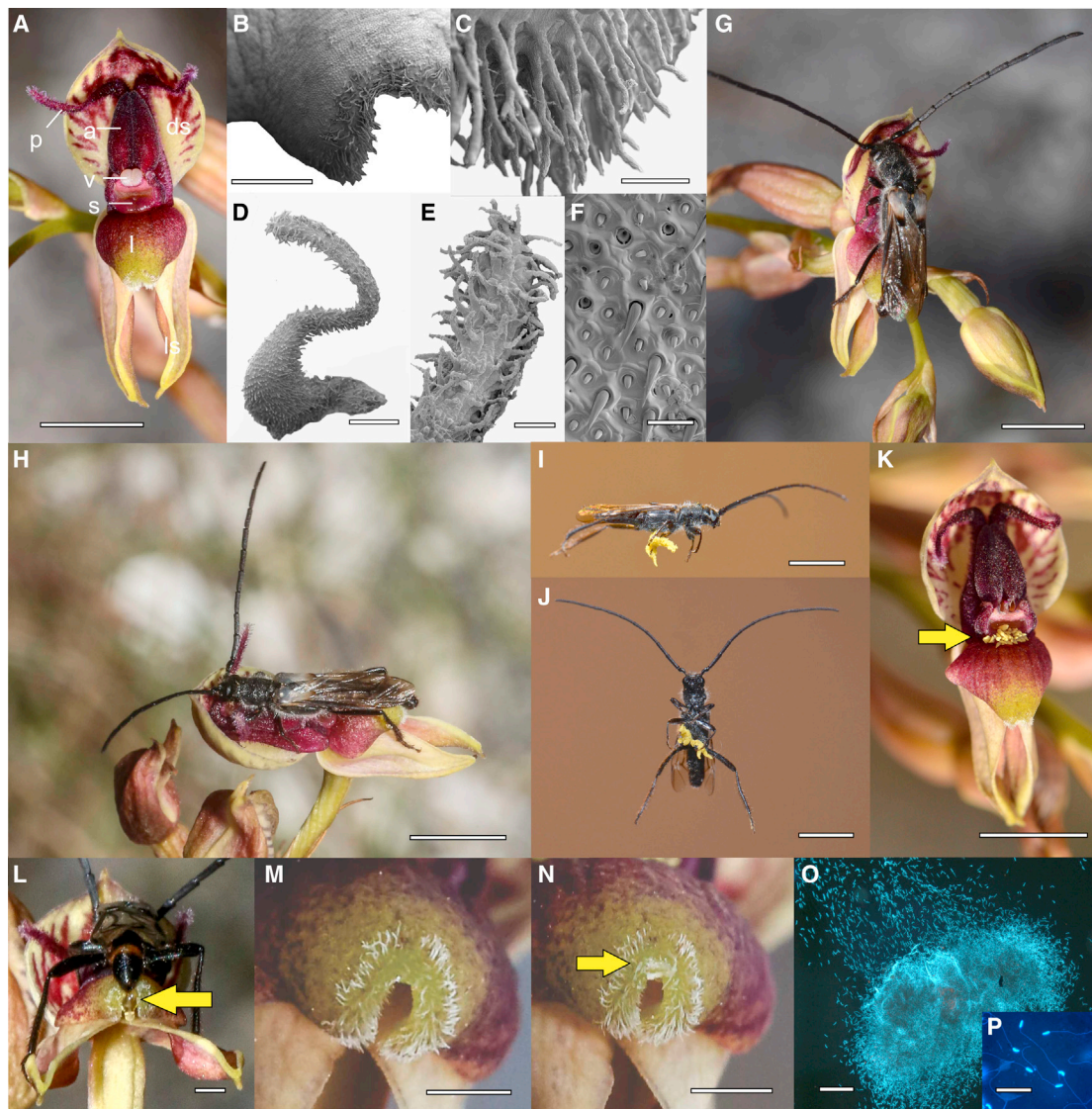


**Figure 1. Floral structure and pollinators of *Disa forficaria***

(A) Unpollinated flower. p, petal; a, anther; ds, dorsal sepal; v, viscidium; s, stigma; l, labellum (=lip); ls, lateral sepal.

(B) Labellum tip showing cleft.

(C) Hairs on the cleft at the tip of the labellum.

(D) Petal.

(E) Hairs on petal.

(F) Sensilla on the antennae of the longhorn beetle *Chorothyse hessei*.

(G and H) *Chorothyse hessei* biting petals of *D. forficaria* and extending the tip of its abdomen into the labellum cleft.

(I and J) *Chorothyse hessei* with pollinaria of *D. forficaria* attached to the sternum.

(K) Flower of *D. forficaria* with pollen massulae (arrow) adhering to the stigma immediately after a visit by *C. hessei*.

(L) *Chorothyse hessei* extending its aedeagus ( $\approx$  penis) into the labellum cleft.

(M) Labellum prior to beetle visit.

(N) Same labellum after a beetle visit with freshly deposited sperm (arrow).

(O) Mass of *C. hessei* sperm removed from the labellum.

(P) Individual *C. hessei* sperm.

Scale bars, 5 mm (A), 500  $\mu$ m (B and D), 100  $\mu$ m (C and P), 200  $\mu$ m (E and O), 20  $\mu$ m (F), 5 mm (G–K), 1 mm (L–N). Image credits: C.C., W.R.L., and S.D.J. See also [Video S1](#).

Despite beetles being the largest order of insects and a well-known group of pollinators, previous evidence for sexual exploitation of beetles by plants has been very limited. Male

*Phyllopertha horticola* scarab beetles have been recorded as secondary pollinators of some European *Ophrys* species and have been shown to be attracted to aliphatic alcohols emitted



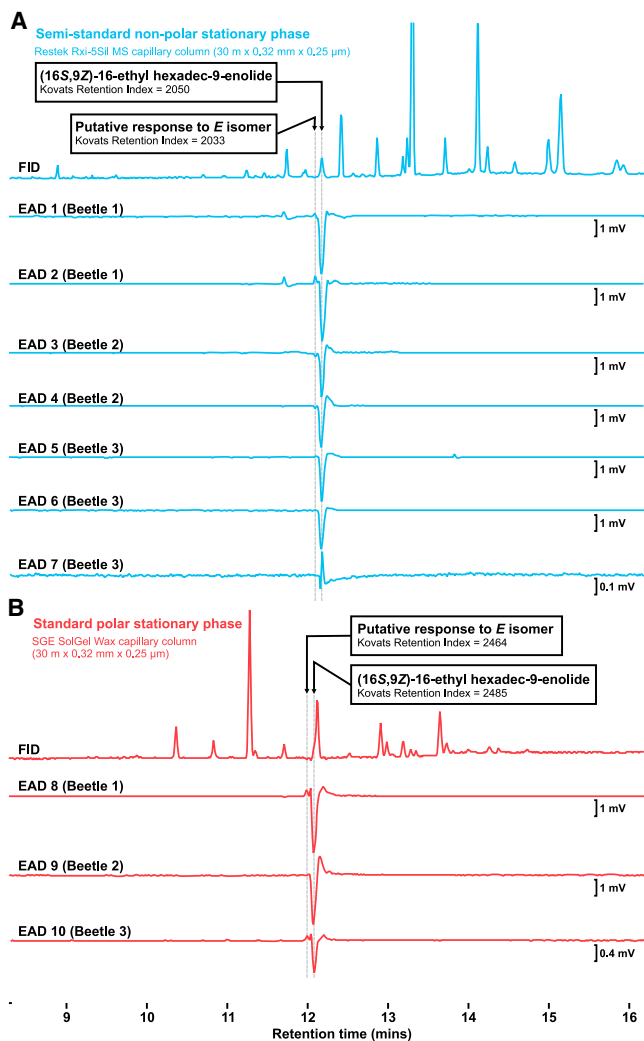


**Figure 2. Electrophysiological response of antennae of male *Chorthyse hessei* beetles to compounds in a solvent extract from a *D. forficaria* flower**

(A) Semi-standard non-polar stationary phase column.

(B) Standard polar stationary phase column.

The main response is to the novel compound (16S,9Z)-16-ethyl hexadec-9-enolide (“disalactone”). The minor response is likely to trace amounts of the (16S,9E) isomer of the same compound, although this was not detected in the mass spectrometry analysis. EAD 7 represents a recording for which the floral extract was diluted by 1,000,000 and the same volume injected as for the remaining EAD traces. Scale bars refer only to EAD traces.

by these flowers.<sup>20</sup> However, it has been suggested that these male beetles may use these aliphatic alcohols as a cue to locate females when they damage plant tissues.<sup>21</sup> The Asian epidendroid orchid *Luisia teres* has been reported to attract male chafer beetles by means of a volatile ester that is also produced by female beetles.<sup>13</sup> However, despite exhibiting occasional copulatory behavior, the chafer beetles also consume nectar on the floral lip. This, taken together with a recent report that female beetles also pollinate flowers in some populations,<sup>12</sup> suggests that the *Luisia* system is transitional between a food-rewarding system and sexual deception.<sup>22</sup>

### Role of volatiles in attraction of beetles

Male *C. hessei* beetles arriving at flowers of *D. forficaria* exhibited slow zig-zag flight paths typical of odor-tracking insects.<sup>23</sup> Antennae from three beetles tested in coupled gas chromatography-flame ionization detection-electroantennographic detection (GC-FID-EAD) experiments with extracts from a flower of the orchid yielded strong and highly repeatable depolarizations (range across all recordings =  $-1.1$  to  $-3.7$  mV) to a single peak (Figure 2). This response was consistent across all replicates with individual beetles (Figure 2). Remarkably, when tested in a single EAD run, antennal responses at this retention time were detectable using injections of 1:1,000 (two EAD runs) and 1:1,000,000 (one EAD run) dilutions of the original floral extract in solvent (Figure 2), but not in additional runs using pure solvent controls. A novel compound, (16S,9Z)-16-ethyl hexadec-9-enolide, corresponding to this retention time was subsequently identified, based on evidence provided by gas chromatography-high-resolution mass spectrometry (GC-HRMS), chemical synthesis, enantiomeric separation techniques, and confirmation of its behavioral effectiveness (Figures 3A–3E, S1, and S2). HRMS data allowed clear dissection of individual ion fragmentation series, and the carbon-carbon double-bond position could be deduced from interruption in the  $C_nH_{n-4}O_2$  ion series caused by a double bond between carbons nine and ten. We propose the trivial name “disalactone” for this compound. A minor antennal response immediately preceding the response to disalactone was also detected in all runs on both columns. There was no detectable peak for this response in our FID chromatograms, but the retention time corresponds to a KRI of 2,033 on the semi-standard non-polar column (Figure 2A) and 2,464 on the polar column (Figure 2B). The retention time of this minor response was subsequently found to correlate closely with the retention time of the *E* isomer of the main bioactive compound on both phases, suggesting that the *E* isomer is present in trace amounts in the floral extract. In electroantennography experiments with puffs of synthesized disalactone and structurally related analogs, we found strong effects of compound type ( $F = 312.1$ ,  $p < 0.0001$ ), but no effect of individual beetle ( $F = 1.69$ ,  $p = 0.23$ ) or interaction of these factors ( $F = 0.95$ ,  $p = 0.48$ ). All tested compounds elicited significantly stronger antennal responses than the solvent control (Figure 3B, note the log scale). Disalactone elicited strong antennal responses (Figure 3A), but similar responses were also detected for (*rac*,9E)-16-ethyl hexadec-9-enolide and (*rac*,8Z)-16-ethyl hexadec-8-enolide (Figure 3B). The other enantiomer of the active compound, (16R,9Z)-16-ethyl hexadec-9-enolide, elicited significantly weaker responses, although still stronger than the responses to the solvent control puffs (Figure 3B).

In four separate field-based bioassays designed to test the behavioral effectiveness of disalactone and structurally related compounds, all of the beetles attracted ( $n = 88$  of which 16 individuals were captured) were males of *C. hessei*. In bioassay 1, which tested a single racemic mixture, nine beetles were attracted to (*rac*,9Z)-16-ethyl hexadec-9-enolide and none were attracted to the solvent control (binomial test,  $p = 0.0038$ ). In bioassay 2, which tested racemic mixtures of various geometric isomers and regioisomers, 32 beetles were attracted to (*rac*,9Z)-16-ethyl hexadec-9-enolide, six beetles to (*rac*,9E)-16-ethyl hexadec-9-enolide, two beetles to the regioisomer (*rac*,8Z)-16-ethyl hexadec-

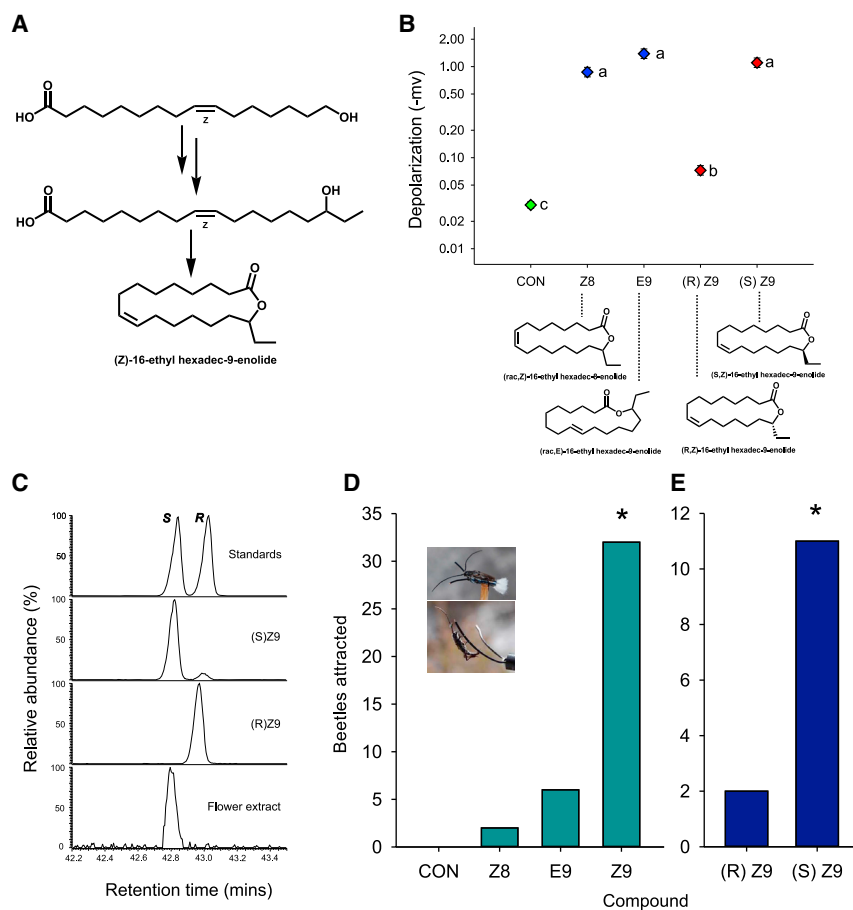


**Figure 3. Bioactivity of semiochemicals extracted from *Disa forficaria* flowers in comparison to structural isomers**

(A) Summary of chemical synthesis of (rac-9Z)-16-ethyl hexadec-9-enolide (for details, see [Supplemental Information](#)).

(B) Electroantennographic (EAG) antennal responses (log-scaled) to disalactone and similar structurally related compounds. CON, acetone solvent control. Means ( $\pm$ SE) that share letters are not significantly different.

(C) Retention of authentic standards of (rac,9Z)-, (16S,9Z)-, and (16R,9Z)-16-ethyl hexadec-9-enolide on a chiral column in comparison to the natural compound present in the floral extract. Section of GC-MS traces is plotted for a  $m/z$  280.07–280.37 mass window as the natural compound is partially obscured by a hydrocarbon peak in the TIC trace.

(D) The numbers of *C. hessei* beetles attracted to disalactone and structurally related compounds. CON, acetone solvent control. Inset: *Chorothyse hessei* beetles on plastic model flowers treated with disalactone. Abdomen curling in the lower image is a typical copulatory behavior.

(E) Beetle discrimination among enantiomers of (Z9)-16-ethyl hexadec-9-enolide.

In (D) and (E), \* $p < 0.05$ , significant difference compared to other compounds in the array. See also [Figures S1](#) and [S2](#), [Data S1](#), and [Video S2](#).

8-enolide, and none to the solvent control (Figure 3D). The beetle choices among isomers in bioassay 2 were significantly non-random ( $G = 45.27$ ,  $p < 0.0001$ ). In bioassay 3, which tested enantiomers, 11 beetles were attracted to (16S,9Z)-16-ethyl hexadec-9-enolide and two beetles were attracted to (16R,9Z)-16-ethyl hexadec-9-enolide (binomial test,  $p = 0.031$ ) (Figure 3E). In bioassay 4, which involved treating dark beads with either disalactone or solvent, 24 beetles were attracted to beads with disalactone and none were attracted to beads with the solvent control (binomial test,  $p < 0.0001$ ). Beetles attracted to beads with disalactone showed frenetic mate-seeking behavior (Video S2). On 3 of the 4 days, the first *C. hessei* individuals attracted to beads treated with disalactone showed prolonged copulatory behavior, which included abdomen bending (Figure 3D, inset). Beetle activity on the orchid and in the bioassays took place only between 11 a.m. and 2 p.m., suggesting a tight diel period for mate searching and mating in this species of beetle.

Our experiments confirm the role of disalactone in attracting male beetles and show that both chirality and the position of the alkene functional group are critically important for eliciting behavioral responses (Figures 3D and 3E). (16S,9Z)-16-ethyl hexadec-9-enolide was by far the most attractive compound in these trials, but we did also record a few beetle attractions to the related *R* enantiomer, as well as to the *E* geometric isomer, and to a related regioisomer (Figures 3D and 3E). Interestingly, all isomers elicited antennal responses, although the responses

to the *R* enantiomer were significantly weaker than responses to disalactone and the other (racemic) isomers tested (Figure 3B). We obtained small antennal responses to the original flower extract at a retention time corresponding exactly to the *E* isomer of disalactone on two different phase columns (Figure 2), leading us to speculate that it is produced in trace amounts that were too small for confirmation using MS. Tight specificity in structure-function of compounds has usually been assumed in sexual deception systems,<sup>14</sup> although recent studies with sexually deceptive *Drakea* orchids and their thynnine wasp pollinators found that in some cases closely related synthetic analogs were as attractive as the natural compound.<sup>15</sup> A subsequent study of the sexually deceptive orchid *Caladenia plicata* and its thynnine wasp pollinator found much tighter specificity, with none of the structurally related isomers that were tested being as attractive as the natural compounds.<sup>24</sup> This suggests that the degree of specificity in the structure-function of bioactive compounds varies between different sexual mimicry systems.

This is the first recorded example of a plant-pollinator interaction mediated by macrocyclic lactones. Macrocyclic lactones are not known among the well-studied sex and aggregation-sex pheromones of Cerambycidae,<sup>25–27</sup> but have been reported without a known function as components of the metasternal gland secretion of the longhorn beetle *Phoracantha synonyma* (Cerambycidae).<sup>28</sup> The exclusive attraction of males ( $n = 99$ ) to both flowers and the synthesized active compound suggests that disalactone is most likely a female-produced sex pheromone of *C. hessei*. This is further supported by the mating behavior observed in the bioassays. It has been suggested

that members of the subfamily Cerambycinae rely exclusively on male-produced volatile aggregation-sex pheromones to bring the sexes together for mating.<sup>27</sup> However, there is some evidence for female-produced pheromones in Cerambycinae,<sup>29</sup> and recent phylogenetic studies have suggested that the subfamily Prioninae, members of which are known to use female-produced sex pheromones, is nested within Cerambycinae.<sup>30</sup> Other lines of evidence consistent with the idea that *C. hessei* females produce volatile sex pheromones include the relatively elongated antennae of the males and the lack of obvious male-specific gland pores on the prothorax that are associated with the production of volatile pheromones.<sup>31</sup> Confirmation that disalactone is a female-produced sex pheromone would require extractions from females, but we did not locate females in the wild despite extensive sweep-netting. The only female ever recorded is a single very old (>50 years) museum specimen. A parallel situation exists in Australia, where putative sex pheromones of some wasp species are known only from the orchids that deploy them for sexual deception of male wasps and have not been confirmed for the fossorial female wasps that have yet to be located.<sup>32</sup>

Disalactone, the macrocyclic lactone described in this study, represents another significant new class of chemical compounds involved in sexual deception in plants. The set of compounds previously known to attract pollinators to other sexually deceptive orchids includes blends of straight-chain alkanes and alkenes, ( $\omega$ -1)-hydroxy and ( $\omega$ -1)-keto carboxylic acids, branched hydroxy esters, cyclohexane-1,3-diones, hydroxylactones, alkyl- and hydroxymethylpyrazines, (methylthio)phenols, and tetrahydrofuran acids.<sup>3,4,13,33</sup> Sexual deception in plants involves a relatively small set of known compounds, but these are often new to science at the time that they are first isolated.<sup>3,4,34</sup>

The biosynthetic origin of disalactone in *D. forficaria* is unknown. In insects, macrocyclic lactones are usually derived from either terpenoid or, more commonly, fatty acid precursors through various processes of chain-shortening, oxidation, and cyclization.<sup>35–37</sup> In plants, oleic acid, which is abundant in plants and could be hydroxylated by CYP450,<sup>38</sup> is a possible precursor for disalactone. Cutin polymer, for example, is built from so-formed  $\omega$ -hydroxylated fatty acid building blocks. But the CYP450 specificity is not limited to the terminal position, and CYP94A1 sub-terminal hydroxylase  $\omega$ -2 was cloned and characterized from *Vicia sativa* L.<sup>39</sup> The plant defense compound volicitin is produced in a similar way.<sup>38</sup> The formed 16-hydroxyoleic acid might be cyclized by an unknown lipase or esterase to form disalactone. Both oxidation and cyclization must be highly enantioselective and effective as only the 16S enantiomer is produced in flowers. Neither saturated lactone nor 16-hydroxyoleic acid were found in our GC-HRMS trace of the flower extract. Related methyl and ethyl stearate peaks were detected with ca. 10%–15% of the abundance of disalactone.

Beetles landed directly on dark plastic beads treated with disalactone, but their approach involved zig-zag flight and they ignored beads treated with control solvent, suggesting that scent cues are key for attraction of beetles. Floral morphology, however, seemed to play an important role in stimulating copulatory behavior once the beetles had located a flower. On the real

flowers, male beetles stroke the filiform petal appendages with their antennae and also occasionally bite them, behavior that is similar to the actual mating behavior described for other longhorn beetles.<sup>17</sup> Other studies of responses of male longhorn beetles to model females have shown that males are very sensitive to the shape and texture of models in terms of initiating copulatory behavior.<sup>40</sup> The dimensions of *D. forficaria* flowers functionally match the size of the beetles and ensure that the genitalia are precisely lined up with the hairy cloaca-like tip of the lip where the beetles were observed to deposit sperm. The exclusive attraction of male *C. hessei* beetles and their obvious sexual behavior (Figures 1G, 1H, and 1L; Video S1), including ejaculation of sperm (Figures 1O and 1P) on the flowers of *D. forficaria*, provide very compelling confirmation of sexual deception in this system.

### Extreme rarity and sexual deception

Prior to the discovery of a single plant in 2018, *D. forficaria* had been last seen in 1966 and was assumed to be extinct.<sup>16</sup> This extreme rarity posed special challenges in this study. It is a testimony to modern analytical methods that we were able to elucidate the structure of the bioactive compound from a single flower without endangering the study plant. The closest other example is a recent study of a rare Australian orchid where extracts of 20 flowers were required to identify the bioactive compounds.<sup>33</sup> When the single known plant of *D. forficaria* disappeared in 2019, we thought that it had become locally extinct. However, when conducting bioassays testing the structure-activity of disalactone and related isomers at the same site in 2020, we were astounded to find that three of the male beetles arriving at our bioassay experiment carried distinctive pollinaria that were subsequently confirmed by DNA barcoding to belong to *D. forficaria*, thus confirming that other plants of the orchid must still exist in the area, even though they could not be located by conventional searching. This is an extraordinary example of how chemical ecology methods can be used to confirm the existence of extremely rare plant species by facilitating the attraction of pollen-carrying insects. Chemical ecology methods also have potential to be used in surveys of sites for the presence of suitable pollinators and thus determine whether habitat is suitable for re-introductions.<sup>33</sup> We found that male *C. hessei* beetles were attracted to disalactone at sites on the Cape Peninsula where the orchid has not been seen for almost a century, thus showing the pollinator is still present and that there is potential for re-establishment of populations.

It has been suggested that sexual deception may have the advantage that it allows plants to achieve pollination even when at very low population densities.<sup>41,42</sup> Plants with conventional floral rewards tend to suffer strong Allee effects at low densities when they become unprofitable to food-seeking animals,<sup>43</sup> but sexually deceptive plants such as *D. forficaria* seem to achieve high levels of pollination and fruit set even at extremely low population densities. It has also been shown that sexually deceptive orchids exhibit particularly efficient transfer of pollen among flowers, presumably because of the high levels of fidelity of male insects.<sup>44</sup> Sexual deception is therefore probably the key explanation for the persistence of *D. forficaria* at extremely low densities.

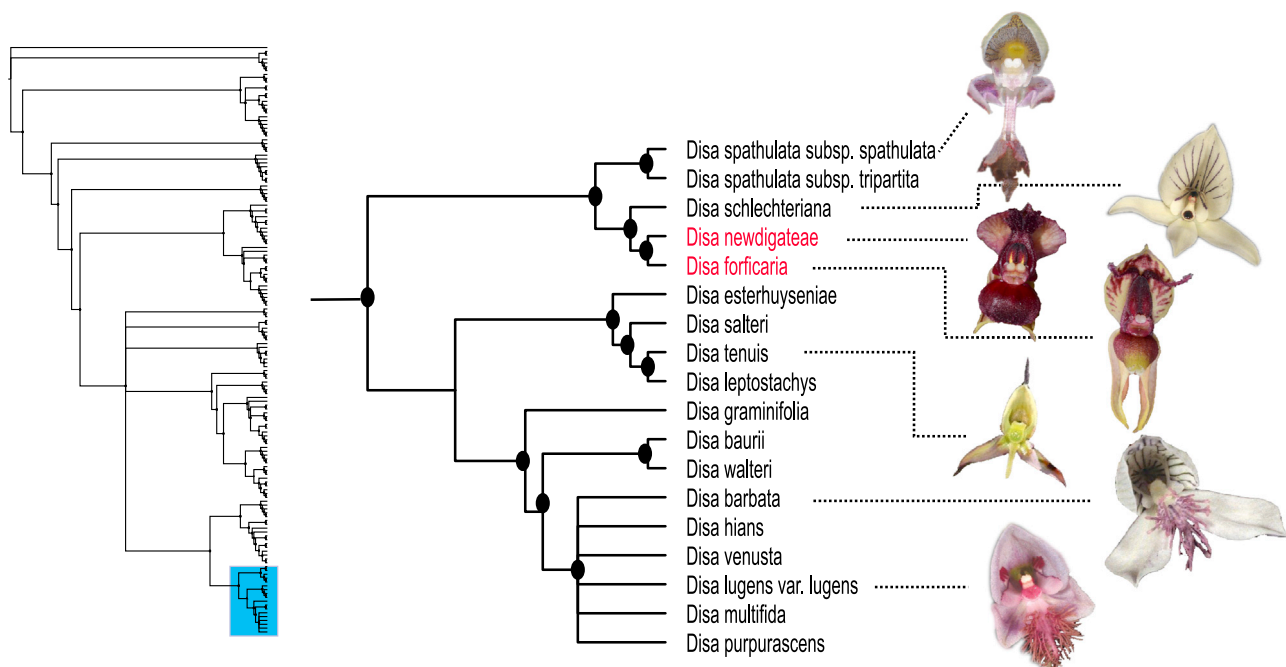


**Figure 4. Phylogenetic position of *Disa forficaria***

Topology of the phylogeny of the genus *Disa* (left) with the clade to which *D. forficaria* belongs shaded in blue and given in greater detail on the right. In the detailed panel, names of food-deceptive species are in black and those of confirmed and putative sexually deceptive taxa are in red. Black ovals indicate nodes that received maximum support in the Bayesian and maximum likelihood analysis. Image credits: W.R.L. and C.C. For details of the overall phylogeny, see [Figure S3](#).

Our phylogenetic analysis ([Figures 4](#) and [S3](#)) shows that *D. forficaria* is most closely related to *D. newdigatae*, another extremely rare species found in a different part of the Cape Floristic Region.<sup>16</sup> *Disa newdigatae* was rediscovered in 2018 after being “lost to science” for almost a century. We recently identified disalactone in extracts taken from flowers of *D. newdigatae*, hinting that it may also be a sexual mimic that also exploits *C. hessei* or another related longhorn beetle species. These two sister species of *Disa* evolved in a clade of species that are food-deceptive, which is consistent with the general trend in orchids for sexual deception to evolve from food deception.<sup>45,46</sup>

This study demonstrates a new type of sexual mimicry in plants involving deception of male longhorn beetles. The beetles show protracted mating behavior that culminated in ejaculation onto the flowers. We show that the beetles are strongly attracted by the novel macrocyclic lactone (16S,9Z)-16-ethyl hexadec-9-enolide (disalactone).

Beetles (Coleoptera) are the most diverse order of animals on Earth (~25% of all known animal species). They are pollinators of at least 34 plant families,<sup>11</sup> and >77,000 species are estimated to visit flowers.<sup>47</sup> Beetles represent the earliest recorded insect pollinators, pre-dating the hymenopteran pollinators by 51 million years.<sup>10</sup> This raises the obvious question of why sexual deception of beetles by plants is apparently so rare, while sexual deception of other insects, such as bees and wasps, has evolved several times.<sup>1,4</sup> One possibility is that beetles are not suitable for transferring pollen, but this is clearly not the case as many plants, including orchids, are effectively pollinated by beetles.<sup>11</sup> A more plausible explanation is that mutations that result in

emission of compounds that match the pheromone systems of beetles are extremely unlikely in plants due to differences in their biochemistry. Thus, mate-seeking male beetles may constitute an enormous niche that is largely unexploited by plants for pollination.

#### STAR★METHODS

Detailed methods are provided in the online version of this paper and include the following:

- KEY RESOURCES TABLE
- RESOURCE AVAILABILITY
  - Lead Contact
  - Materials Availability
  - Data and Code Availability
- EXPERIMENTAL MODEL AND SUBJECT DETAILS
  - Study species
- METHOD DETAILS
  - Pollinator behavior
  - Electrophysiology
  - Gas chromatography
  - Mass spectrometry
  - Chemical synthesis
  - Field bioassays
  - Phylogeny and pollen barcoding
- QUANTIFICATION AND STATISTICAL ANALYSIS
  - Electrophysiology
  - Bioassays
  - Phylogenetic analysis



## SUPPLEMENTAL INFORMATION

Supplemental information can be found online at <https://doi.org/10.1016/j.cub.2021.03.037>.

## ACKNOWLEDGMENTS

This paper is dedicated to the memory of Wittko Francke (1940–2020), who played a major role in developing our understanding of the chemistry of floral deception. We thank Georg Pohnert and Daniel Stetin, Friderich Schiller University Jena for running samples on the GC-Q-Exactive system. We thank Pierre-Olivier Maquart for assistance in the identification of *Chorothisse hessei*. Fran Jordaan, Liz Hutton, Garth Hutton, Sandy Jenkin, Pat Miller, and Lee Burman are greatly thanked for their generous help in facilitating our field research at Hermanus over several years. We also thank Carl Holdt, Karen Pagel, Paul Venter, Marthinus Vosloo, Herbert Stärker, Craig Peter, Terry Trinder-Smith, and Susie Cunningham for their generous assistance. Sampling took place under CapeNature permit 0056-AAA007-00010. S.D.J. and A. Shuttleworth were supported by the National Research Foundation of South Africa (grant numbers 46372, 90691, and 127037). J.F.C. was supported by a National Research Foundation Research Career Advancement Fellowship (grant number 91442). The Max Planck Society is acknowledged for financial support for identification work and chemical synthesis.

## AUTHOR CONTRIBUTIONS

C.C. discovered the orchid-beetle interaction. C.C. and W.R.L. made field observations and conducted bioassays. J.F.C. made field observations and identified beetles. A. Shuttleworth performed the coupled GC-electroantennography and J.W. did the chemical synthesis. A. Svatoš identified the candidate compound using mass spectrometry. B.B. performed the phylogenetic analysis with assistance from W.R.L. S.D.J. made field observations, conducted bioassays, performed electron microscopy, analyzed beetle sperm, and wrote the paper with input from all the authors.

## DECLARATION OF INTERESTS

The authors declare no competing interests

Received: December 4, 2020

Revised: February 13, 2021

Accepted: March 10, 2021

Published: March 25, 2021

## REFERENCES

- Johnson, S.D., and Schiestl, F.P. (2016). *Floral mimicry* (Oxford University Press).
- Gaskett, A.C. (2011). Orchid pollination by sexual deception: pollinator perspectives. *Biol. Rev. Camb. Philos. Soc.* **86**, 33–75.
- Peakall, R., Wong, D.C.J., Bohman, B., Flematti, G., and Pichersky, D. (2020). Floral volatiles for pollinator attraction and speciation in sexually deceptive orchids. In *Biology of Plant Volatiles*, E. Pichersky, and N. Dudareva, eds. (CRC Press), pp. 271–298.
- Bohman, B., Flematti, G.R., Barrow, R.A., Pichersky, E., and Peakall, R. (2016). Pollination by sexual deception-it takes chemistry to work. *Curr. Opin. Plant Biol.* **32**, 37–46.
- Schiestl, F.P., Ayasse, M., Paulus, H.F., Löfstedt, C., Hansson, B.S., Ibarra, F., and Francke, W. (1999). Orchid pollination by sexual swindle. *Nature* **399**, 421–422.
- Schiestl, F.P., Peakall, R., Mant, J.G., Ibarra, F., Schulz, C., Franke, S., and Francke, W. (2003). The chemistry of sexual deception in an orchid-wasp pollination system. *Science* **302**, 437–438.
- Phillips, R.D., Scaccabarozzi, D., Retter, B.A., Hayes, C., Brown, G.R., Dixon, K.W., and Peakall, R. (2014). Caught in the act: pollination of sexually deceptive trap-flowers by fungus gnats in *Pterostylis* (Orchidaceae). *Ann. Bot.* **113**, 629–641.
- Blanco, M.A., and Barboza, G. (2005). Pseudocopulatory pollination in *Iepanthes* (orchidaceae: pleurothallidinae) by fungus gnats. *Ann. Bot.* **95**, 763–772.
- Martel, C., Francke, W., and Ayasse, M. (2019). The chemical and visual bases of the pollination of the Neotropical sexually deceptive orchid *Telipogon peruvianus*. *New Phytol.* **223**, 1989–2001.
- Bao, T., Wang, B., Li, J., and Dilcher, D. (2019). Pollination of Cretaceous flowers. *Proc. Natl. Acad. Sci. USA* **116**, 24707–24711.
- Bernhardt, P. (2000). Convergent evolution and adaptive radiation of beetle-pollinated angiosperms. *Plant Syst. Evol.* **222**, 293–320.
- Sugiura, N., Matsumura, S., and Yokota, M. (2020). Beetle pollination of *Luisia teres* (Orchidaceae) and implications of a geographic divergence in the pollination system. *Plant Species Biol.* **36**, 52–59.
- Wakamura, S., Arakaki, N., Moriyama, D., Kanayama, S., Oike, M., Kimura, A., Wajima, S., Ono, H., and Yasui, H. (2020). Does the orchid *Luisia teres* attract its male chafer pollinators (Scarabaeidae: *Protaetia pryeri pryeri*) by sexual deception? *Chemoecology* **30**, 49–57.
- Bohman, B., Karton, A., Flematti, G.R., Scaffidi, A., and Peakall, R. (2018). Structure-activity studies of semiochemicals from the spider orchid *Caladenia plicata* for sexual deception. *J. Chem. Ecol.* **44**, 436–443.
- Bohman, B., Karton, A., Dixon, R.C.M., Barrow, R.A., and Peakall, R. (2016). Parapheromones for thynnine wasps. *J. Chem. Ecol.* **42**, 17–23.
- Liljedal, W.R., and Johnson, S.D. (2012). *The Cape Orchids: A Regional Monograph of the Orchids of the Cape Floristic Region* (Sandstone Editions).
- Michelsen, A. (1963). Observations on the sexual behaviour of some longicorn beetles, subfamily Lepturinae (Coleoptera, Cerambycidae). *Behaviour* **22**, 152–166.
- Gaskett, A.C., Winnick, C.G., and Herberstein, M.E. (2008). Orchid sexual deceit provokes ejaculation. *Am. Nat.* **171**, E206–E212.
- Quentin, R.M., and Villiers, A. (1971). Révision de *Psebiini* (col. Cerambycidae Cerambycinae). *Ann. Soc. Entomol. Fr.* **7**, 3–38.
- Borg-Karlson, A.-K. (1989). Attraction of *Phyllopertha horticola* (Coleoptera, Scarabaeidae) males to fragrance components of *Ophrys* flowers (Orchidaceae, section Fuciflorae). *Entomol. Tidskr.* **109**, 105–109.
- Ruther, J. (2004). Male-biased response of garden chafer, *Phyllopertha horticola* L., to leaf alcohol and attraction of both sexes to floral plant volatiles. *Chemoecology* **14**, 187–192.
- Arakaki, N., Yasuda, K., Kanayama, S., Jitsuno, S., Oike, M., and Wakamura, S. (2016). Attraction of males of the cupreous polished chafer *Protaetia pryeri pryeri* (Coleoptera: Scarabaeidae) for pollination by an epiphytic orchid *Luisia teres* (Asparagales: Orchidaceae). *Appl. Entomol. Zool.* **51**, 241–246.
- Murlis, J., Elkinton, J.S., and Carde, R.T. (1992). Odor plumes and how insects use them. *Annu. Rev. Entomol.* **37**, 505–532.
- Xu, H., Bohman, B., Wong, D.C.J., Rodriguez-Delgado, C., Scaffidi, A., Flematti, G.R., Phillips, R.D., Pichersky, E., and Peakall, R. (2017). Complex sexual deception in an orchid is achieved by co-opting two independent biosynthetic pathways for pollinator attraction. *Curr. Biol.* **27**, 1867–1877.e5.
- Hanks, L.M., and Millar, J.G. (2016). Sex and aggregation-sex pheromones of Cerambycid beetles: basic science and practical applications. *J. Chem. Ecol.* **42**, 631–654.
- Allison, J.D., Borden, J.H., and Seybold, S.J. (2004). A review of the chemical ecology of the Cerambycidae (Coleoptera). *Chemoecology* **14**, 123–150.
- Millar, J.G., and Hanks, L.M. (2017). *Chemical ecology of cerambycids. In Cerambycidae of the World: Biology and Pest Management*, Q.F. Wang, ed. (CRC Press), pp. 161–208.
- Moore, B.P., and Brown, W.V. (1976). The chemistry of the metasternal gland secretion of the eucalypt longicorn *Phoracantha synonyma* (Coleoptera: Cerambycidae). *Aust. J. Chem.* **29**, 1365–1374.



29. Itami, J.K., and Craig, T.P. (1989). Life-history of *Styloxus bicolor* (Coleoptera, Cerambycidae) on *Juniperus monosperma* in northern Arizona. *Ann. Entomol. Soc. Am.* **82**, 582–587.
30. Wang, J., Dai, X.Y., Xu, X.D., Zhang, Z.Y., Yu, D.N., Storey, K.B., and Zhang, J.Y. (2019). The complete mitochondrial genomes of five longicorn beetles (Coleoptera: Cerambycidae) and phylogenetic relationships within Cerambycidae. *PeerJ* **7**, e7633.
31. Ray, A.M., Lacey, E.S., and Hanks, L.M. (2006). Predicted taxonomic patterns in pheromone production by longhorned beetles. *Naturwissenschaften* **93**, 543–550.
32. Bohman, B., Jeffares, L., Flematti, G., Byrne, L.T., Skelton, B.W., Phillips, R.D., Dixon, K.W., Peakall, R., and Barrow, R.A. (2012). Discovery of tetra-substituted pyrazines as semiochemicals in a sexually deceptive orchid. *J. Nat. Prod.* **75**, 1589–1594.
33. Bohman, B., Tan, M.M.Y., Phillips, R.D., Scaffidi, A., Sobolev, A.N., Moggach, S.A., Flematti, G.R., and Peakall, R. (2020). A specific blend of drakolide and hydroxymethylpyrazines: An unusual pollinator sexual attractant used by the endangered orchid *Drakaea micrantha*. *Angew. Chem. Int. Ed. Engl.* **59**, 1124–1128.
34. Franke, S., Ibarra, F., Schulz, C.M., Twele, R., Poldy, J., Barrow, R.A., Peakall, R., Schiestl, F.P., and Francke, W. (2009). The discovery of 2,5-dialkylcyclohexan-1,3-diones as a new class of natural products. *Proc. Natl. Acad. Sci. USA* **106**, 8877–8882.
35. Schulz, S., and Hötling, S. (2015). The use of the lactone motif in chemical communication. *Nat. Prod. Rep.* **32**, 1042–1066.
36. Schulz, S., Yildizhan, S., Stritzke, K., Estrada, C., and Gilbert, L.E. (2007). Macrolides from the scent glands of the tropical butterflies *Heliconius cydno* and *Heliconius pacheus*. *Org. Biomol. Chem.* **5**, 3434–3441.
37. Vanderwel, D., Johnston, B., and Oehlschlager, A.C. (1992). Cucujolide biosynthesis in the merchant and rusty grain beetles. *Insect Biochem. Mol. Biol.* **22**, 875–883.
38. Pinot, F., and Beisson, F. (2011). Cytochrome P450 metabolizing fatty acids in plants: characterization and physiological roles. *FEBS J.* **278**, 195–205.
39. Kandel, S., Morant, M., Benveniste, I., Blée, E., Werck-Reichhart, D., and Pinot, F. (2005). Cloning, functional expression, and characterization of CYP709C1, the first sub-terminal hydroxylase of long chain fatty acid in plants. Induction by chemicals and methyl jasmonate. *J. Biol. Chem.* **280**, 35881–35889.
40. Fukaya, M., and Honda, H. (1996). Reproductive biology of the yellow-spotted longicorn beetle, *Psacothoa hilaris* (Pascoe) (Coleoptera: Cerambycidae) 0.4. Effects of shape and size of female models on male mating behaviors. *Appl. Entomol. Zool.* **31**, 51–58.
41. Peakall, R. (1990). Responses of male *Zaspilothynnus trilobatus* Turner wasps to females and the sexually deceptive orchid it pollinates. *Funct. Ecol.* **4**, 159–167.
42. Peakall, R., and Beattie, A.J. (1996). Ecological and genetic consequences of pollination by sexual deception in the orchid *Caladenia tentaculata*. *Evolution* **50**, 2207–2220.
43. Groom, M.J. (1998). Allee effects limit population viability of an annual plant. *Am. Nat.* **151**, 487–496.
44. Scopece, G., Cozzolino, S., Johnson, S.D., and Schiestl, F.P. (2010). Pollination efficiency and the evolution of specialized deceptive pollination systems. *Am. Nat.* **175**, 98–105.
45. Inda, L.A., Pimentel, M., and Chase, M.W. (2012). Phylogenetics of tribe Orchideae (Orchidaceae: Orchidoideae) based on combined DNA matrices: inferences regarding timing of diversification and evolution of pollination syndromes. *Ann. Bot.* **110**, 71–90.
46. Weston, P.H., Perkins, A.J., Indsto, J.O., and Clements, M.A. (2014). Phylogeny of Orchidaceae tribe Diurideae and its implications for the evolution of pollination systems. In *Darwin's Orchids: Then and Now*, P. Bernhardt, and R. Meier, eds. (Chicago University Press), pp. 92–154.
47. Ollerton, J. (2017). Pollinator diversity: distribution, ecological function, and conservation. *Annu. Rev. Ecol. Evol. Syst.* **48**, 353–376.
48. Singh, A.N., Mhaskar, V.V., and Dev, S. (1978). Chemistry of lac resin - VIII: synthesis of jalaric ester-I, possible key compound in elaboration of lac resin by *Laccifer lacca* kerr. *Tetrahedron* **34**, 595–598.
49. Babu, K.V., and Sharma, G.V.M. (2008). Total synthesis of patulolide C and 11-epipatulolide C. *Tetrahedron Asymmetry* **19**, 577–583.
50. Hall, T.A. (1999). BioEdit: a user-friendly biological sequence alignment editor and analysis program for Windows 95/98/NT. *Nucleic Acids Symp. Ser.* **41**, 95–98.
51. Maddison, W.P., and Maddison, D.R. (2019). *Mesquite: a modular system for evolutionary analysis*, 2.75 Edition.
52. Ronquist, F., Teslenko, M., van der Mark, P., Ayres, D.L., Darling, A., Höhna, S., Larget, B., Liu, L., Suchard, M.A., and Huelsenbeck, J.P. (2012). MrBayes 3.2: efficient Bayesian phylogenetic inference and model choice across a large model space. *Syst. Biol.* **61**, 539–542.
53. Hood, M.E. (1994). Poptools version 2.6.2 (CSIRO).
54. Stein, S.E. (1995). Chemical substructure identification by mass spectral library searching. *J. Am. Soc. Mass Spectrom.* **6**, 644–655.
55. Stamatakis, A. (2014). RAxML version 8: a tool for phylogenetic analysis and post-analysis of large phylogenies. *Bioinformatics* **30**, 1312–1313.
56. Rambaut, A., Drummond, A.J., Xie, D., Baele, G., and Suchard, M.A. (2018). Posterior summarization in Bayesian phylogenetics using Tracer 1.7. *Syst. Biol.* **67**, 901–904.
57. Shuttleworth, A., and Johnson, S.D. (2020). Using two confluent capillary columns for improved gas chromatography-electroantennographic detection (GC-EAD). *Entomol. Exp. Appl.* **168**, 191–197.
58. Johnson, S.D., Hobbhahn, N., and Bytebier, B. (2013). Ancestral deceit and labile evolution of nectar production in the African orchid genus *Disa*. *Biol. Lett.* **9**, 20130500.
59. Bytebier, B., Bellstedt, D.U., and Linder, H.P. (2007). A molecular phylogeny for the large African orchid genus *Disa*. *Mol. Phylogenet. Evol.* **43**, 75–90.
60. Doyle, J.J., and Doyle, J.L. (1987). A rapid DNA isolation procedure for small quantities of fresh leaf tissue. *Phytochem. Bull.* **19**, 11–15.

## STAR★METHODS

## KEY RESOURCES TABLE

REAGENT or RESOURCE	SOURCE	IDENTIFIER
Chemicals, Peptides, and Recombinant Proteins		
(16 <i>R</i> ,9 <i>Z</i> )-16-Ethyl hexadec-9-enolide	Synthesized for this paper	N/A
(16 <i>R</i> ,9 <i>Z</i> )-16-Hydroxyoctadec-9-enoic acid	Synthesized for this paper	CAS number: 278601-95-9
(16 <i>S</i> ,9 <i>Z</i> )-16-Acetoxyoctadec-9-enoic acid	Synthesized for this paper	N/A
(16 <i>S</i> ,9 <i>Z</i> )-16-Ethyl hexadec-9-enolide (“disalactone”)	Synthesized for this paper	N/A
(16 <i>S</i> ,9 <i>Z</i> )-16-Hydroxyoctadec-9-enoic acid	Synthesized for this paper	CAS number: 1254593-03-7
(16 <i>Z</i> )-16-((tetrahydro-2 <i>H</i> -pyran-2-yl)oxy)hexadec-8-enoic acid	Synthesized for this paper	N/A
(8 <i>Z</i> )-16-Hydroxyhexadec-8-enoic acid	Synthesized for this paper	N/A
(8 <i>Z</i> )-16-Oxohexadec-8-enoic acid	Synthesized for this paper	N/A
(9 <i>E</i> )-16-Hydroxyhexadec-9-enoic acid	Synthesized for this paper according to Singh et al. <sup>48</sup>	CAS number: 17278-80-7
(9 <i>E</i> )-16-Oxohexadec-9-enoic acid	Synthesized for this paper	CAS number: 142666-22-6
(9 <i>Z</i> )-16-Hydroxyhexadec-9-enoic acid	Synthesized for this paper according to Singh et al. <sup>48</sup>	CAS number: 1619-68-7
(9 <i>Z</i> )-16-Oxohexadec-9-enoic acid	Synthesized for this paper	N/A
( <i>rac</i> ,8 <i>Z</i> )-16-Ethyl hexadec-8-enolide	Synthesized for this paper	N/A
( <i>rac</i> ,8 <i>Z</i> )-16-Hydroxyoctadec-8-enoic acid	Synthesized for this paper	N/A
( <i>rac</i> ,9 <i>E</i> )-16-Ethyl hexadec-9-enolide	Synthesized for this paper	N/A
( <i>rac</i> ,9 <i>E</i> )-16-Hydroxyoctadec-9-enoic acid	Synthesized for this paper	N/A
( <i>rac</i> ,9 <i>Z</i> )-16-Acetoxyoctadec-9-enoic acid	Synthesized for this paper	N/A
( <i>rac</i> ,9 <i>Z</i> )-16-Ethyl hexadec-9-enolide	Synthesized for this paper	N/A
( <i>rac</i> ,9 <i>Z</i> )-16-Hydroxyoctadec-9-enoic acid	Synthesized for this paper	CAS number: 141522-76-1
2-Methyl-6-nitrobenzoic anhydride (MNBA)	Sigma Aldrich	CAS number: 434935-69-0; 681059
4- <i>N,N</i> -Dimethylaminopyridine (DMAP)	Fluka	CAS number: 1122-58-3; 29224
8-((Tetrahydro-2 <i>H</i> -pyran-2-yl)oxy)octanal	Synthesized for this paper according to Babu and Sharma <sup>49</sup>	CAS number: 57221-80-4
8-Bromooctanoic acid	Sigma Aldrich	CAS number: 17696-11-6; 257583
Acetic anhydride	Sigma Aldrich	CAS number: 108-24-7; 242845
Acetone	Fluka	CAS number: 67-64-1; 34480
Acetone	Honeywell, Riedel de Haën, Chromasolv for HPLC	CAS number: 67-64-1; 34850
C7-C40 Saturated Alkanes Standard	Sigma-Aldrich, SUPELCO	49452-U
<i>Candida antarctica</i> lipase, immobilized (2.9 U/mg)	Sigma Aldrich	73940
Carbon dioxide	Sodastream	N/A
DAPI	Sigma-Aldrich	CAS number: 28718-90-3
Dess-Martin Periodinane	Sigma Aldrich	CAS number: 87413-09-0; 274623
Dichloromethane	Carl Roth GmbH	CAS number: 75-09-2; KK47.1
Dichloromethane	Honeywell, Riedel de Haën, Chromasolv for HPLC	CAS number: 75-09-2; 34856
Diethylether, anhydrous	Sigma Aldrich	CAS number: 60-29-7; 346136
Ethylacetate	Carl Roth GmbH	CAS number: 141-78-6; T164.1
Ethylmagnesium bromide solution in diethylether	Sigma Aldrich	CAS number: 925-90-6; 189871
Lithium hydroxide monohydrate	Sigma Aldrich	CAS number: 1310-66-3; 402974

(Continued on next page)

<b>Continued</b>		
REAGENT or RESOURCE	SOURCE	IDENTIFIER
Methanol	Merck	CAS number: 67-56-1; 1.06018
<i>n</i> -Hexane	Carl Roth GmbH	CAS number: 110-54-3; 4723.2
Pyridine	Sigma Aldrich	CAS number: 110-86-1; 360570
Ringer (tablets)	Merck	1.15525.0001
Silica gel 60 (230-400 mesh)	Carl Roth GmbH	CAS number: 7631-86-9; P091.3
Sodium bis(trimethylsilyl)amide, 40% solution in THF	Sigma Aldrich	CAS number: 1070-89-9; 80631
Tetrahydrofuran, anhydrous	Sigma Aldrich	CAS number: 109-99-9; 401757
Toluene	Carl Roth GmbH	CAS number: 108-88-3; 7115.1
Triphenylphosphine	Sigma Aldrich	CAS number: 603-35-0; T84409
<b>Critical Commercial Assays</b>		
DNeasy Plant Mini Kit	QIAGEN	Catalogue number: 69104
KAPA3G Plant PCR Kit	Kapa Biosystems	KK7251
<b>Deposited Data</b>		
Combined alignment (trnLF, matK, ITS)	This paper	<a href="http://doi.org/10.5281/zenodo.4450105">http://doi.org/10.5281/zenodo.4450105</a>
Voucher information	This paper	<a href="http://doi.org/10.5281/zenodo.4539824">http://doi.org/10.5281/zenodo.4539824</a>
ITS GenBank accessions	This paper	<i>Disa esterhuyseniae</i> (GenBank: MT703013)
		<i>Disa forficaria</i> (GenBank: MT703014)
		<i>Disa leptostachys</i> (GenBank: MT703015)
		<i>Disa newdigateae</i> (GenBank: MT703016)
Plastid GenBank accessions	This paper	<i>trnL-F</i>
		<i>Disa esterhuyseniae</i> (GenBank: MT740818)
		<i>Disa forficaria</i> (GenBank: MT740816)
		<i>Disa leptostachys</i> (GenBank: MT740819)
		<i>Disa newdigateae</i> (GenBank: MT740817)
		<i>matK</i>
		<i>Disa esterhuyseniae</i> (GenBank: MT731942)
		<i>Disa forficaria</i> (GenBank: MT731940)
		<i>Disa leptostachys</i> (GenBank: MT731943)
		<i>Disa newdigateae</i> (GenBank: MT731941)
<b>Software and Algorithms</b>		
BioEdit v7.2	50	<a href="https://bioedit.software.informer.com/7.2/">https://bioedit.software.informer.com/7.2/</a>
FigTree v 1.4.4.	<a href="http://tree.bio.ed.ac.uk/software/figtree/">http://tree.bio.ed.ac.uk/software/figtree/</a>	<a href="https://github.com/rambaut/figtree/releases/tag/v1.4.4">https://github.com/rambaut/figtree/releases/tag/v1.4.4</a>
GcEad 2014 v. 1.2.5 (2014-05-03)	Syntech	<a href="http://gcead.sourceforge.net">http://gcead.sourceforge.net</a>
IBM SPSS Statistics 25	IBM	<a href="https://www.ibm.com/products/spss-statistics?lnk=hpmps_bupr&amp;lnk2=learn;">https://www.ibm.com/products/spss-statistics?lnk=hpmps_bupr&amp;lnk2=learn;</a> RRID: SCR_019096
Mesquite 3.61	51	<a href="http://www.mesquiteproject.org/">http://www.mesquiteproject.org/</a>
MrBayes 3.2.7a	52	<a href="https://www.phylo.org/">https://www.phylo.org/</a>
Poptools 2.6.2	53	<a href="https://www.maa.org/press/periodicals/loci/resources/poptools">https://www.maa.org/press/periodicals/loci/resources/poptools</a>
NIST Spectral Library v. 20	54	<a href="https://www.nist.gov/system/files/documents/srd/NIST1a11Ver2-0Man.pdf">https://www.nist.gov/system/files/documents/srd/NIST1a11Ver2-0Man.pdf</a>
RAxML 8.2.12	55	<a href="https://www.phylo.org/">https://www.phylo.org/</a>
Tracer v1.7	56	<a href="https://github.com/beast-dev/tracer/releases/tag/v1.7.1">https://github.com/beast-dev/tracer/releases/tag/v1.7.1</a>
Xcalibur software v. 3.1 SP4	Thermo Scientific	<a href="https://www.thermofisher.com/order/catalog/product/OPTON-30965#/OPTON-30965">https://www.thermofisher.com/order/catalog/product/OPTON-30965#/OPTON-30965</a>

(Continued on next page)

**Continued**

REAGENT or RESOURCE	SOURCE	IDENTIFIER
Other		
Restek Rxi-5Sil MS capillary column	Restek	13624
SGE SolGel Wax capillary column	Trajan Scientific and Medical	054788
Zebtron ZB-SemiVolatiles capillary column	Phenomenex	7HG-G027-11
J/W Cyclosil-B capillary column	Agilent	112-6632

**RESOURCE AVAILABILITY****Lead Contact**

Further information and requests for resources should be directed to and will be fulfilled by the Lead Contact, Steven D. Johnson ([Johnsonsd@ukzn.ac.za](mailto:Johnsonsd@ukzn.ac.za)).

**Materials Availability**

This study did not generate new unique reagents

**Data and Code Availability**

Experimental data are available in the published article. DNA sequences can be downloaded from GenBank (<https://www.ncbi.nlm.nih.gov/genbank/>); ITS accession numbers: *Disa esterhuyseniae* (MT703013), *Disa forficaria* (MT703014), *Disa leptostachys* (MT703015), *Disa newdigateae* (MT703016); Plastid accession numbers, trnL-F: *Disa esterhuyseniae* (MT740818), *Disa forficaria* (MT740816), *Disa leptostachys* (MT740819), *Disa newdigateae* (MT740817), matK: *Disa esterhuyseniae* (MT731942), *Disa forficaria* (MT731940), *Disa leptostachys* (MT731943), *Disa newdigateae* (MT731941).

**EXPERIMENTAL MODEL AND SUBJECT DETAILS****Study species**

*Disa forficaria* Bolus (Figure 1A) is an exceedingly rare southern African orchid species known from just nine records of 11 plants since its discovery in the early nineteenth century.<sup>16</sup> No more than two plants have ever been found at any one locality in a given year. A single plant of *D. forficaria* was discovered in 2016 near Hermanus in the southwestern part of the Cape Floristic Region. Prior to this, the last sighting of *D. forficaria* was 50 years previously, in 1966, and the species had thus been considered possibly extinct.<sup>16</sup> When the single known plant disappeared in 2019 we thought that it had become locally extinct, as we had searched thoroughly for additional plants nearby. However, when conducting bioassays in 2020 to test the active compound identified in this study, we found that three of the male beetles arriving at our bioassay experiment carried fresh pollinaria of *D. forficaria*, confirming that one or more other plants of the orchid still exist in the area. The pollinaria of *D. forficaria* are distinctive on account of their very large viscidium and short caudicle, but we also confirmed their identity using DNA barcoding (see below).

The flowers of this species face directly upward and exhibit a densely hairy, kidney-shaped lip with a cleft at its distal tip (Figures 1B and 1C), and narrow, minutely hairy petals which curl backward and resemble insect antennae (Figures 1D and 1E). The horizontal orientation of the two petals and the lip create a landing platform, measuring approximately 9 mm in length from the cleft tip of the lip to the strongly recurved bend of the antennae-like petals. During their summer leafless state, plants produce up to 13 inconspicuous flowers, each measuring 17.2 mm by 7.2 mm, on a ca. 30 cm tall reed-like stem. Typically, only one receptive flower is open at a time, with each flower remaining open for one to two days. Along with our observations, herbarium records from several localities show that fruits are produced from most of the flowers on an inflorescence, even though the plants lack a mechanism for self-pollination, and are thus completely reliant on pollinators. Flowers were examined for visible traces of nectar but no floral reward was detected. Fruits were formed from 9 of the 13 flowers produced by the *D. forficaria* plant in 2016.

*Chorothisse hessei*<sup>19</sup> (Cerambycidae: Cerambycinae) is a longhorn beetle endemic to the Cape Floristic Region. The sexes appear to be similar in coloration and size; males we captured had a mean ( $\pm$ s.e) body length of  $9.88 \pm 0.24$  mm (range 7.8–12.3 mm,  $n = 19$ ), while the body length of the female type specimen was given as 12 mm.<sup>19</sup> However, strong sexual dimorphism is evident in the antennae, with the antennae of males we captured measuring  $12.33 \pm 0.43$  mm ( $n = 14$ ) which is 24% longer than their mean body length, while the antenna of the female type specimen is approximately half of its body length.<sup>19</sup> Both sexes show drastically reduced elytra, which is typical of wasp-mimicking cerambycids and a common feature among diurnal species of the subfamily Cerambycinae.

**METHOD DETAILS****Pollinator behavior**

Pollinator observations, timed to coincide with the opening of flowers, took place over a total of eight days in March 2016 and four days in March 2018 (no flowering occurred in 2017 and the plant has not appeared aboveground since early 2019). These



observations typically took place in warm conditions between 10 h00 and 15 h00. We photographed and video-recorded the behavior of *C. hessei* beetles (the only insects observed on the flowers) and captured representative specimens for identification and for electrophysiological experiments (see below). We recorded whether these beetle visitors removed and deposited pollen and if they exhibited copulatory behavior. To determine if visitors ejaculate on flowers, we removed a putative sperm sample from the lip cleft of a flower with fine forceps immediately after a visit by *C. hessei*. After 24 h of storage in an Eppendorf tube at 8°C, the sample was placed on a slide in standard PBS buffer with 1: 1000 DAPI (4',6-diamidino-2-phenylindole) stain and examined under a fluorescence microscope.

### Electrophysiology

We conducted gas chromatography-electroantennographic detection coupled with flame ionisation detection (GC-FID-EAD) experiments to identify which volatile compounds in the floral extract could be involved in the attraction of *C. hessei* beetles to *D. forficaria* flowers. These experiments followed methods described in Shuttleworth and Johnson.<sup>57</sup> Briefly, we used a gas chromatograph fitted with two capillary columns (a polar SGE SolGel Wax column and a semi-standard non-polar Restek Rxi-5Sil MS column, both 30 m × 0.32 mm ID × 0.25 μm film thickness). Both columns were connected to the same four-way effluent splitter and the remaining two ports from the splitter delivered effluent to the beetle antenna and the FID respectively.<sup>57</sup> For each run, one column was used as the analytical column while the second column delivered make-up gas at the split for EAD. By switching parameters for each column, this confluent configuration allowed successive runs on different stationary phases with the same antenna. Initial electrophysiology experiments were conducted in March 2018 using three male *C. hessei* beetles collected from *D. forficaria* flowers. Beetles were transported to the laboratory in a cooler bag, then stored in a fridge and used for testing over the following two days. Floral volatiles were collected by soaking a single *D. forficaria* flower in 500 μl of dichloromethane (Honeywell, Riedel-de Haën, Chromasolv, ≥ 99.8%) for 60 min. The attractiveness of this extract to beetles was verified in the field before proceeding. Beetles were anaesthetized with CO<sub>2</sub> and an antenna removed at the base with cutting forceps. The tip of the antenna was also removed, and the antenna was mounted between capillaries filled with ¼ strength Ringer solution (Merck, Germany) for EAD recordings. EAD recordings were made with apparatus supplied by Ockenfels Syntech (Buchenbach, Germany) using GcEad 2014 v.1.2.5 (2014-05-03) software. For each beetle, we obtained three EAD recordings (two on the semi-standard non-polar phase and one on the polar phase), each using 5 μl injections of the floral extract. Having established the presence of a consistent strong antennal response to one of the peaks, we also explored the lower detection threshold using 5 μl injections of the floral extract diluted by 1000 (a single EAD run on each phase) and by 1 000 000 (a single EAD run on the semi-standard non-polar phase). We also tested pure dichloromethane (a single EAD run on the semi-standard non-polar phase) to confirm that the response was not due to a contaminant in our solvent. Linear (non-isothermal) *n*-alkane Kováts retention indices (KRI) were calculated for active compounds.

This response (Figure 2) was consistent across all replicates with individual beetles and was still detected on runs for which the floral extract was diluted by 1000 and by 1 000 000 (Figure 2). A minor antennal response immediately preceding this large depolarisation was also detected in all runs on both columns. There was no detectable peak for this response in our FID chromatograms, but the retention time corresponds to a KRI of 2033 on the semi-standard non polar column and 2464 on the polar column. The retention time of this minor response was subsequently found to correlate closely with the retention time of the *E* isomer of the main bioactive compound on both phases. Minor antennal responses at retention times corresponding to KRI of 1855 and 1944 were also obtained in runs on the semi-standard non-polar column. These were consistent across all runs.

After synthesizing the putative active compound (16*S*,9*Z*)-16-ethyl hexadec-9-enolide (disalactone) (see Chemical synthesis below), we conducted electroantennography (EAG) experiments to confirm antennal responses by male *C. hessei* beetles to it. To explore the effects of minor changes to the structure or absolute configuration of the active compound, we also tested the antennal responses to the other enantiomer of the active compound, (16*R*,9*Z*)-16-ethyl hexadec-9-enolide, the other geometric isomer of the active compound, (*rac*,9*E*)-16-ethyl hexadec-9-enolide, and to a similar regioisomer of the active compound, (*rac*,8*Z*)-16-ethyl hexadec-8-enolide. Antennae were mounted as described above and placed in a stream of filtered and humidified air flowing through an 8 mm ID glass tube at a flow rate of ca. 4 l per min controlled by a Syntech CS55 Stimulus Controller. Test compounds were delivered to the antenna as discrete puffs (0.5 s duration) introduced to the glass tube ca. 10 cm away from the antenna and carried onto the antennal preparation by the humidified air. For each puff, 10 μl of the test compound diluted to 1 in 2000 in acetone (Honeywell, Riedel-de Haën, Chromasolv, ≥ 99.8%) or pure acetone (as a control to correct for antennal responses to the solvent) was pipetted onto a small piece of filter paper placed in the mouth of a Pasteur pipette and immediately connected to the stimulus controller and puffed onto the antenna. The four test compounds were puffed onto the antenna in succession, starting and ending with control solvent puffs and the duration of each set of test puffs was less than four minutes. This was repeated 18 times (eight times with an antenna from one beetle and five times with antennae from each of the remaining two beetles) and the sequence of compounds in between the solvent puffs was randomized. Antennal depolarisations corresponding to each puff were recorded using GcEad 2014 v.1.2.5 (2014-05-03) software.

### Gas chromatography

In order to determine the chemical structure of the bioactive compound detected through GC-FID-EAD, an aliquot (1 μl) of the dichloromethane *D. forficaria* flower extract described above was mixed with 1 μl of diluted C8 - C30 hydrocarbon standards in hexane and injected on a ZB-SemiVolatiles column (5% phenyl, 95% dimethylpolysiloxane; 30 m × 0.25 mm ID × 0.25 μm film thickness, with a 10 m pre-column retention gap; Phenomenex, Aschaffenburg, Germany) using splitless injection at 250°C. The

sample was eluted with He (1 mL/min) using a temperature gradient starting at 40°C, held for 2 min, then heated to 200°C at a rate of 10°C/min, held for 10 min, heated to 250°C at a rate of 10°C/min, held for 5 min and finally raised to 320°C at a rate of 10°C/min and held for 5 min. Eluted compounds were ionized using electron ionization at 70 eV. Ions were detected with an Orbitrap analyzer at 120 000 mass resolution. Three lock mass ions from the column background were used to achieve the best mass data accuracy ( $m/z$  73.0468, 133.0136, and 207.0324). This experiment was performed on a GC-Q-Exactive system (Thermo Scientific). Data were analyzed using Xcalibur software v. 3.1 SP4.

Chirality was determined using chemical synthesis of enantiomeric lactones and retention times of individual enantiomers were compared to the native sample. Chiral analyses were performed on a GC-MS Trace (Thermo) using 112-6632 Agilent J/W Cyclosil-B (30 m × 0.25 mm ID × 0.245 μm film thickness) chiral column and a temperature gradient starting at 40°C, held for 2 min, then heated to 100°C at a rate of 10°C/min, and then heated to 240°C at a rate of 3°C/min and held for 10 min.

### Mass spectrometry

Inspection of accurate mass spectra for a peak at a retention time of 12.50 min corresponding to a KRI of 2050 (the value where antennal activity was detected; [Figure 2](#)) showed a small molecular peak at  $m/z$  280.23971 ([Figure S1](#)) with calculated molecular composition  $C_{18}H_{32}O_2$  (delta 0.5520 mmu from calculated value). It was accompanied by an intense ion series of  $m/z$  109, 95, 81, 67 corresponding to molecular composition of  $C_8H_{13}^+$ ,  $C_7H_{11}^+$ ,  $C_6H_9^+$  and  $C_5H_7^+$ , respectively characterized for aliphatic dienes or cycloalkenes. Small but informative ion peaks at  $m/z$  262.22923 ( $C_{18}H_{30}O$ )  $M^{++} - H_2O$  and  $m/z$  251.20055 ( $C_{16}H_{27}O_2$ )  $M^{++} - C_2H_5^+$  pointed to hydroxyl or carbonyl groups and ethyl branching. The first hit for the determined molecular formulae was linoleic acid, but the KRI for this compound did not match and preferential ethyl radical loss is not likely. The other possibility was a macrocyclic lactone and  $\omega$ -ethyl branching, which led to the putative 16-ethyl hexadecenolide structure. Double bond position could be deduced from a series of losses from  $m/z$  251: 238.19268 ( $C_{15}H_{26}O_2$ ) 251 -  $CH^+$ ; 224.17701 ( $C_{14}H_{24}O_2$ ) 251 -  $C_2H_3^+$ ; 210.16132 ( $C_{13}H_{22}O_2$ ) 251 -  $C_3H_5^+$ ; 196.14569 ( $C_{12}H_{20}O_2$ ) 251 -  $C_4H_7^+$ ; 182.13002 ( $C_{11}H_{18}O_2$ ) 251 -  $C_5H_9^+$ ; 168.11439 ( $C_{10}H_{16}O_2$ ) 251 -  $C_6H_{11}^+$ ; 154.09876 ( $C_9H_{14}O_2$ ) 251 -  $C_7H_{13}^+$ ; low 140.08315 ( $C_8H_{12}O_2$ ) 251 -  $C_8H_{15}^+$  and not continuing, stopping at  $\Delta 9$  position. The final proposed structure for synthesis was 16-ethyl hexadec-9-enolide. Double bond geometry and chirality at C16 was further determined by chemical synthesis ([Figures S2](#) and [3A](#)) and comparing KRI of the original sample and the prepared isomers ([Figure 3C](#)). As  $\Delta 8$  is also a plausible explanation of the MS data, 16-ethyl hexadec-8-enolide was also prepared ([Figure S2](#)). Final confirmation of the identification was derived from GC-EAD and behavioral experiments. Due to the small amounts of sample available, we were not able to perform a derivatization reaction to determine double bond position more rigorously (e.g., with  $I_2$ /DMDS treatment) and the structure was determined from one GC-HRMS injection. The natural compound showed very high enantiomeric purity (over 95% e.e.) and its retention time corresponded to the 16S-enantiomer ([Figure 3C](#)).

### Chemical synthesis

The putative bioactive compound, identified by a combination of electrophysiology and mass spectrometry, and structurally related molecules were synthesized from the respective 16-hydroxyhexadecenoic acids (8Z, 9E or 9Z), which were either obtained by Wittig-reaction (8Z) or from aleuritic acid (9E and 9Z) using the protocol of Singh et al.<sup>48</sup> After oxidation to the aldehydes, the ethyl-sidechain was introduced via a Grignard-reaction to yield the 16-hydroxyoctadecenoic acids. The lactones were then formed via Shiina macro-lactonization using 2-methyl-6-nitrobenzoic anhydride (MNBA) as the condensation reagent. The stereoisomers of (9Z)-16-ethyl hexadec-9-enolide were obtained via enzymatic resolution of the acetylated (9Z)-16-hydroxy-octadec-9-enoic acid using *Candida antarctica* lipase. According to chiral GC-MS-analysis, the enantiomeric excess of (16R,9Z)-16-ethyl hexadec-9-enolide was 99% while (16S,9Z)-16-ethyl hexadec-9-enolide (disalactone) was obtained in 85%ee. The specific rotation values were found to be  $[\alpha]_{589}^{20} = +3.2$  for the R-enantiomer and  $[\alpha]_{589}^{20} = -2.2$  for the S-enantiomer. They were determined via polarimetry using solutions of 3 mg/mL in *n*-hexane. The detailed procedures and analytical data can be found in [Figure S2](#).

### Field bioassays

We conducted a series of bioassays to test the behavioral effectiveness of the putative bioactive compound (16S,9Z)-16-ethyl hexadec-9-enolide (see Results). We also tested the structure-activity of closely-related molecules. For these experiments, we used 1:2000 dilutions of compounds in acetone (Honeywell, Riedel-de Haën, Chromasolv,  $\geq 99.8\%$ ). Each choice consisted of 2 mL of test solution placed in an open 5 mL smoked glass vial into which a ca. 8 cm length of slender dry reed was inserted to serve as a landing platform for insects. Insects that landed on the reeds or flew or crawled to within 10 cm of the entrance to the vial were considered to be attracted to the compound. Vials in the array were placed 50 cm apart. In bioassay 1, conducted over two days at the Hermanus site, we presented a two-way choice between (*rac*,9Z)-16-ethyl hexadec-9-enolide (the putative bioactive compound in a racemic mix) and an acetone control. In bioassay 2, conducted over two days at the Hermanus site, we presented a four-way choice between pure acetone (the negative control), (*rac*,9Z)-16-ethyl hexadec-9-enolide (the putative bioactive compound in a racemic mix), (*rac*,9E)-16-ethyl hexadec-9-enolide (the geometric isomer of the bioactive compound), and (*rac*,9Z)-16-ethyl hexadec-8-enolide (a regioisomer of the bioactive compound). In bioassay 3, conducted over two days at the Hermanus site, we presented a two-way choice between the S and R enantiomers of the bioactive compound. In bioassay 4, conducted over four days at a site on the Cape Peninsula, 85 km from Hermanus, we presented disalactone to further test: 1. if only male beetles are attracted to the compound, 2. if a landing platform induced mating behavior, and 3. if the beetle pollinators still occurred at this site where the orchid is presumed to have become extinct. For this bioassay, we placed a ca. 5 μL droplet of 1:2000 disalactone in acetone on model

flowers placed on reeds of the same length as those in the other bioassays and consisting of dark plastic beads (10 mm by 3–4 mm) with “antennae” of plastic-coated wire and a small tuft of hairs approximating the hairy lip of the flower at one end of the model. Model flowers treated with a droplet of pure acetone served as controls.

### Phylogeny and pollen barcoding

We sequenced leaf material of *D. forficaria* to establish its placement in the broader *Disa* phylogeny and thus be able to compare its pollination system with those of its close relatives, and also to determine whether it evolved in a rewarding or non-rewarding clade of *Disa*.<sup>58</sup> As the species had not been seen since 1966, it was not included in the study by Bytebier et al.<sup>59</sup> Furthermore, *Disa newdigateae* L.Bolus, another extremely rare species sharing similar floral traits and considered closely related to *D. forficaria*, was unexpectedly rediscovered in 2018 and could thus also be included in the phylogeny. Prior to this, *D. newdigateae* was known only from three collections and last seen in the 1930s.<sup>16</sup> Plant material of two other rare members of *Disa* section *Trichochila*, to which *D. forficaria* is assigned, namely *Disa esterhuyseniae* Schelpe ex H.P.Linder and *Disa leptostachys* Sond., currently considered a synonym of *Disa tenuis* Lindl., were also included in the phylogenetic analysis. Due to the extreme rarity of these species, collection of entire plants was deemed inappropriate and we therefore used high-resolution photographs and spirit-preserved single flowers as vouchers which are lodged in the Bews Herbarium (NU) and Compton Herbarium (NBG). Small amounts of fresh leaf material of the species were dried in silica gel and stored at  $-20^{\circ}\text{C}$ . Total DNA was purified with the DNeasy Plant Mini Kit (QIAGEN, Hilden, Germany). Two chloroplast markers were amplified: the pseudo-gene maturase K (*matK* - including the non-coding *trnK* intron), and the tRNA-Leu gene and the *trnL* and *trnL-F* intergenic spacer (= *trnL* and *trnL-F*). In addition, one nuclear region was amplified: the internal transcribed spacers (ITS). PCR amplification, primers and sequencing were exactly as described in Bytebier et al.<sup>59</sup>

Phylogenetic analysis (Figures 4 and S3) showed that *D. forficaria* is sister to *D. newdigateae* and is, as was predicted by morphological analysis, nested in the non-rewarding clade *Disa* section *Trichochila*. *Disa forficaria* belongs to a sub-clade that includes *Disa spathulata* (L.f.) Sw., which has a short floral spur and is bee-pollinated, and *Disa schlechteriana* Bolus, which has a long floral spur and is putatively pollinated by long-proboscid flies.<sup>16</sup> The sister relationship between *D. forficaria* and *D. newdigateae*, as well as the sister relationship of this clade to *D. schlechteriana*, received maximum support in the Bayesian, as well as the Maximum Likelihood analyses (Figure S3).

DNA from one pollinarium, retrieved from a longhorn beetle caught during the 2020 field bioassay study, was extracted using a slightly modified version of the CTAB protocol.<sup>60</sup> The single pollinarium was crushed with one Tungsten bead in a QIAGEN TissueLyser II at 30 Hz for 3 min, after which 100  $\mu\text{l}$  standard CTAB buffer was added and the mixture was incubated at  $65^{\circ}\text{C}$  for 30 min. DNA was extracted with chloroform-isoamyl alcohol, precipitated with ice-cold isopropanol and cleaned with wash buffer (70% ethanol, 10mM ammonium acetate). The DNA was air-dried and re-suspended in 50  $\mu\text{l}$  water. Four  $\mu\text{l}$  was used in 50  $\mu\text{l}$  standard PCR reaction to amplify the nuclear ITS region. The sequence obtained was a 100% match for the ITS sequence of *Disa forficaria*.

## QUANTIFICATION AND STATISTICAL ANALYSIS

### Electrophysiology

Antennal depolarisations (- mV) resulting from each test compound and the solvent controls (Data S1A) were compared using a log-normal generalized linear mixed models (Data S1B) with beetle, isomer type and their interaction as fixed effects, antennal recording as the subject, puff position as the repeated-measure (the covariance matrix was auto-regressive) implemented in SPSS 25 (IBM) Means were compared using Šidák posthoc tests.

### Bioassays

Data from the bioassays (Figures 3D and 3E) for two-way choices were analyzed using exact binomial tests and for four-way choices were analyzed using G tests, implemented in Poptools ver 2.6.2.<sup>53</sup> Each replicate was a beetle individual that flew or crawled to within 10 cm of a test vial.

### Phylogenetic analysis

The sequences obtained were inserted into the matrix used in Bytebier et al.<sup>59</sup> and were manually aligned in BioEdit v7.0.1. Bayesian phylogenetic analysis was performed under the best model parameters using MrBayes on XSEDE (v3.2.7a) available in the CIPRES Science Gateway V. 3.3. The analysis, using two independent parallel runs, consisted of 10 million MCMC generations, and was sampled every 1000 generations. We assessed convergence between runs by checking the effective sample size (ESS > 200) of each parameter and the log-likelihood (LnL) values, using Tracer v1.7. We discarded the first 25% of the trees as the burn-in period. A Maximum Likelihood (ML) analysis was performed using RAxML available in the CIPRES Science Gateway, using the GTRCAT substitution model and 1,000 bootstrap replicates for statistical support. The ML and Bayesian trees were then visualized and edited using FigTree v 1.4.2.